Supporting Information for

High Conduction Band Inorganic Layers for Distinct Enhancement of Electrical Energy Storage in Polymer Nanocomposites

Yingke Zhu[1], Zhonghui Shen[2], Yong Li[3], Bin Chai[1], Jie Chen[1], Pingkai Jiang[1], Xingyi Huang[1, *]

[1]Department of Polymer Science and Engineering, Shanghai Key Laboratory of Electrical Insulation and Thermal Ageing, State Key Laboratory of Metal Matrix Composites, Shanghai Jiao Tong University, Shanghai 200240, People's Republic of China

[2]State Key Laboratory of Advanced Technology for Materials Synthesis and Processing, Center of Smart Materials and Devices, Wuhan University of Technology, Wuhan 430070, People's Republic of China

[3]Institute of Applied and Physical Chemistry and Center for Environmental Research and Sustainable Technology, University of Bremen, Bremen 28359, Germany

*Corresponding author. E-mail: xyhuang@sjtu.edu.cn (Xingyi Huang)

Supplementary Tables and Figures

Table S1 The values of parameters used in this simulation at 298 K and 300 MV m^{-1}

Parameters	Values in matrix	Values in filler
Schottky barrier (eV)	1.0	/
Trap Depth ξ (eV)	0.12 (at interfaces)	/
Electron mobility ($cm^2/V{\cdot}s$)	9×10^{-11}	10 (in plane) 0.01 (out of plane)
Dielectric constant	16	5

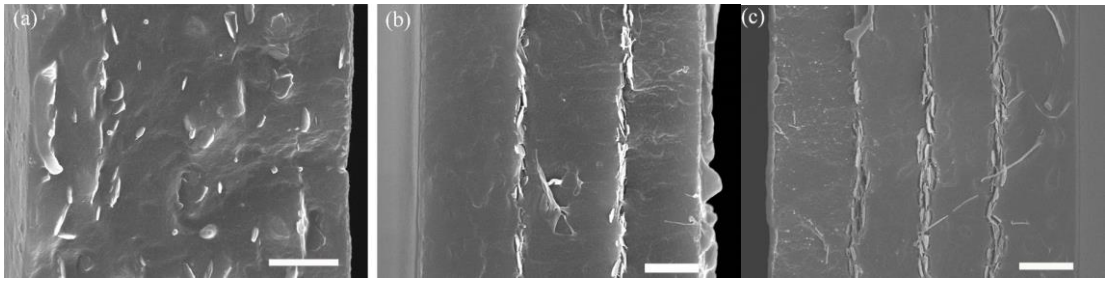

Fig. S1 SEM images of **a** BNNS random dispersed composite, **b** composite with two aligned BNNS layers, **c** composite with three aligned BNNS layers(all scalr bars are 2 μm)

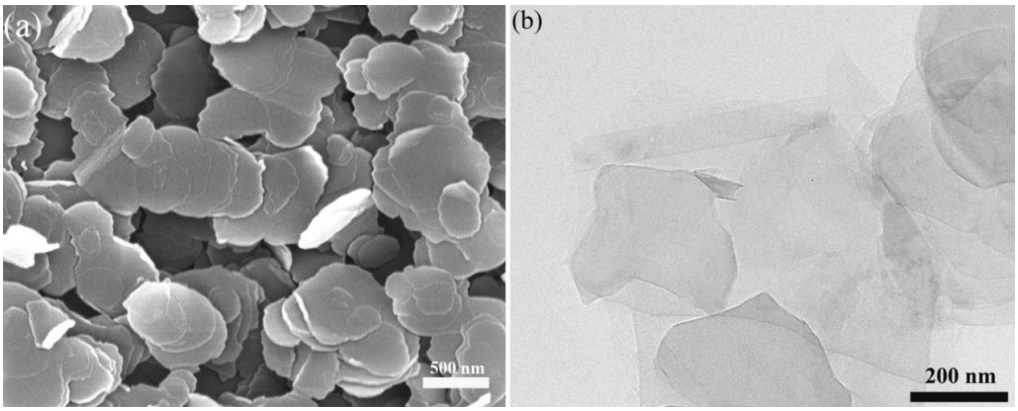

Fig. S2 a SEM and **b** TEM image of BNNSs

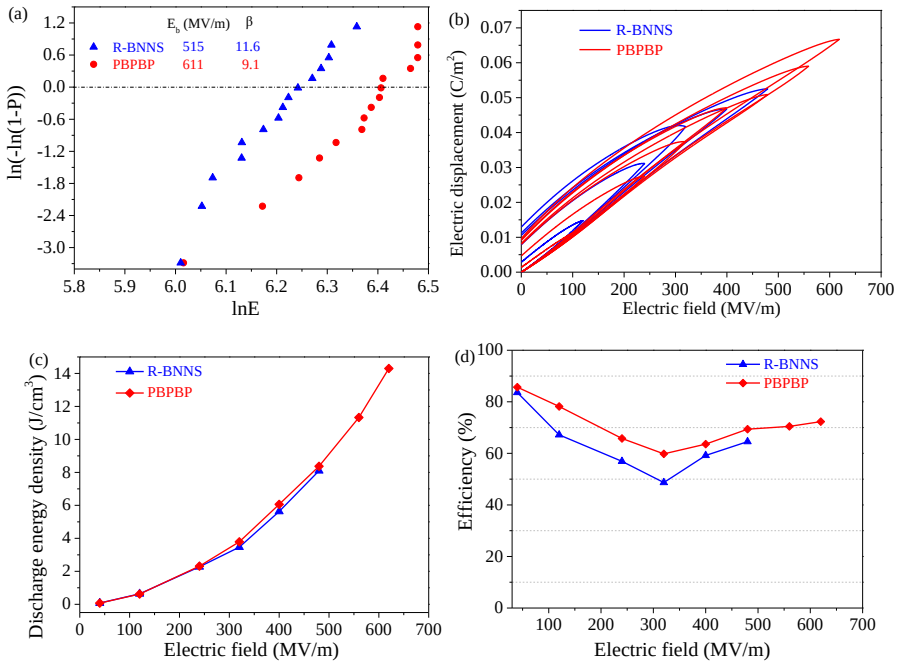

Fig. S3 Comparison of **a** Weibull breakdown strength, **b** D-E loops, **c** discharged energy density, and **d** charge-discharge efficiency of R-BNNS and PBPBP

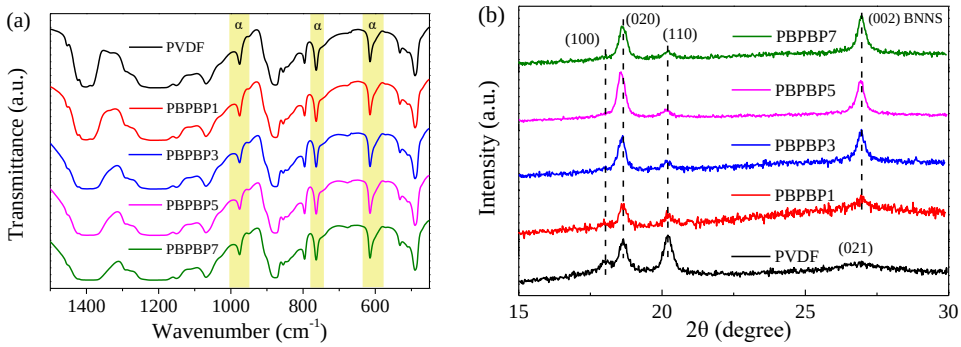

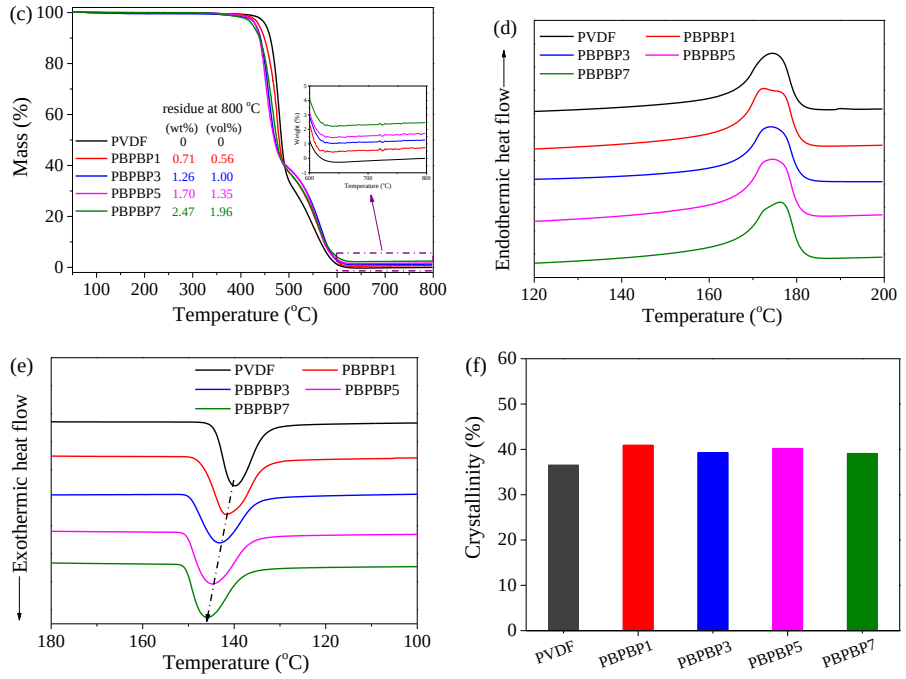

Fig. S4 a FT-IR, **b** XRD, **c** TG, **d** DSC heating, **e** DSC cooling, and **f** crystallinity spectra of PVDF, and PBPBP films

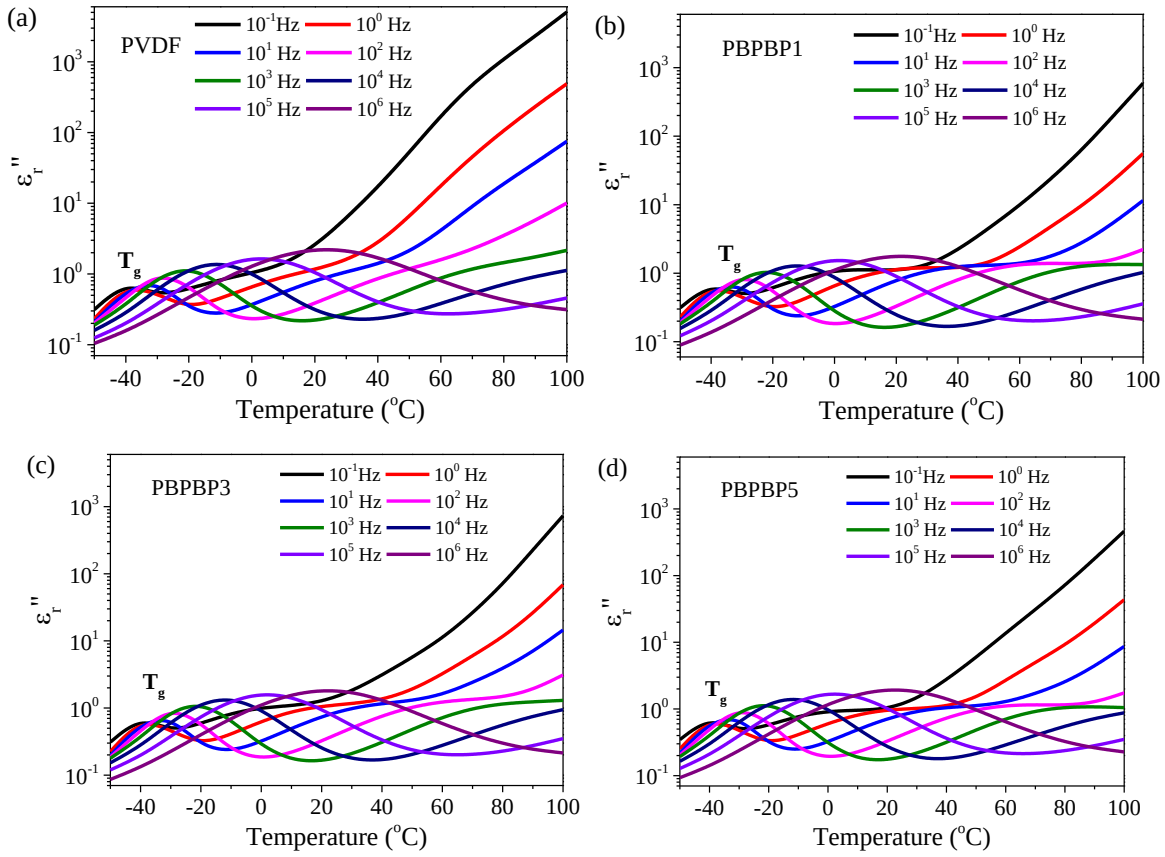

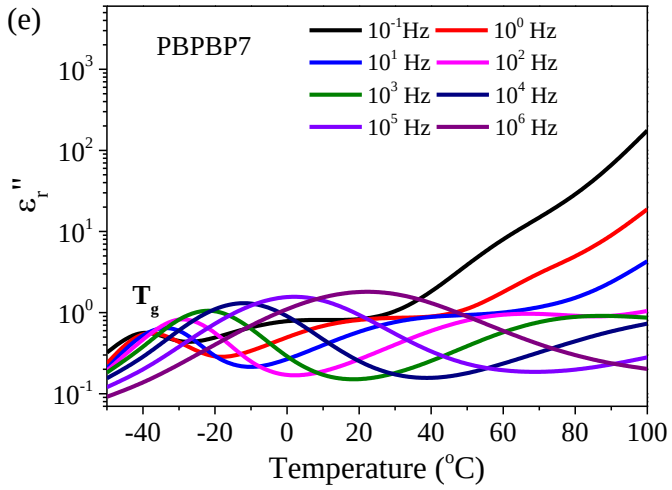

Fig. S5 Imaginary part of dielectric constant (ε_r'') of **a** PVDF, **b** PBPBP1, **c** PBPBP3, **d** PBPBP5, **e** PBPBP7 under various temperature

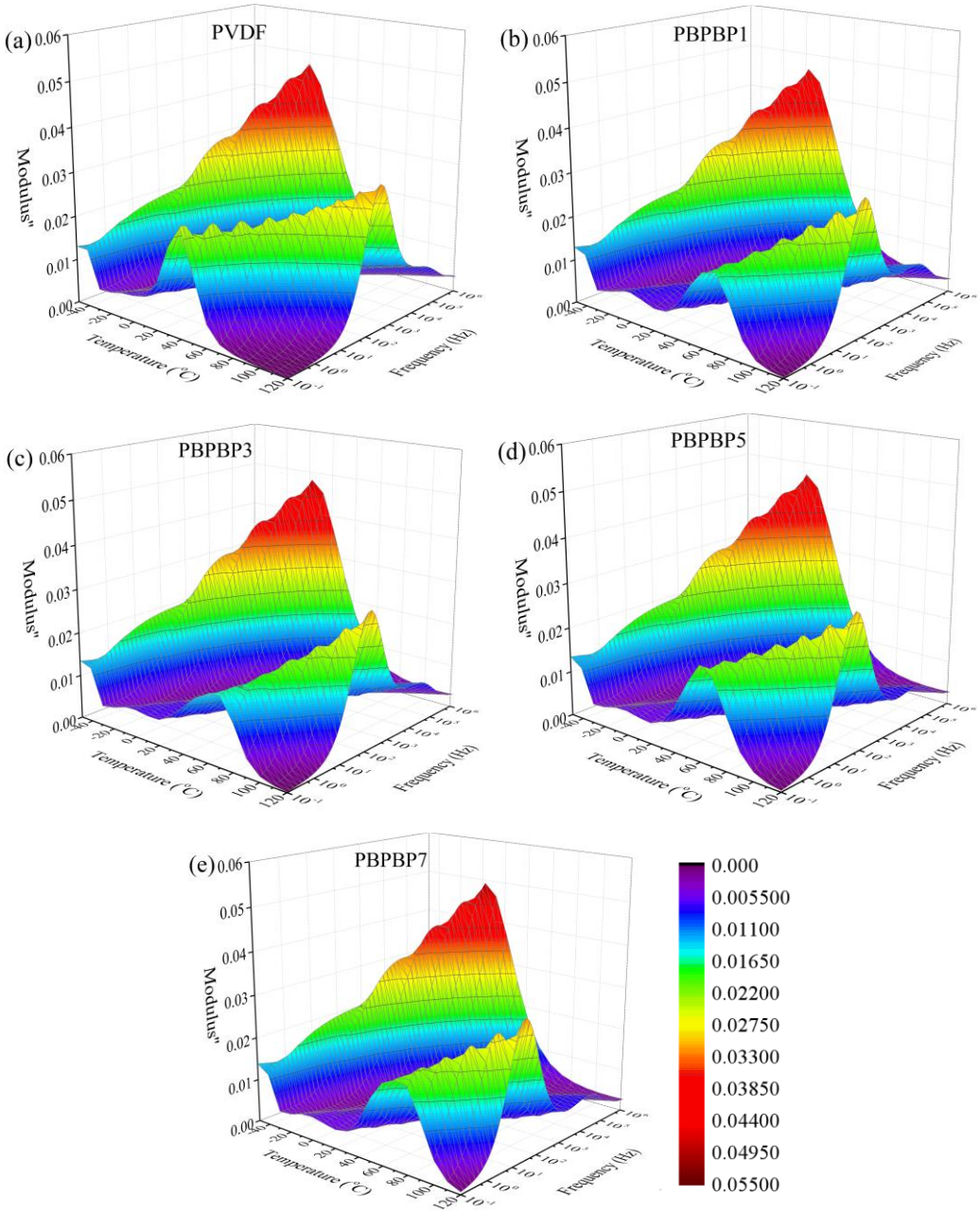

Fig. S6 Frequency dependance of the imaginary part of electric modulus (M'') of PVDF and PBPBP films under various temperature

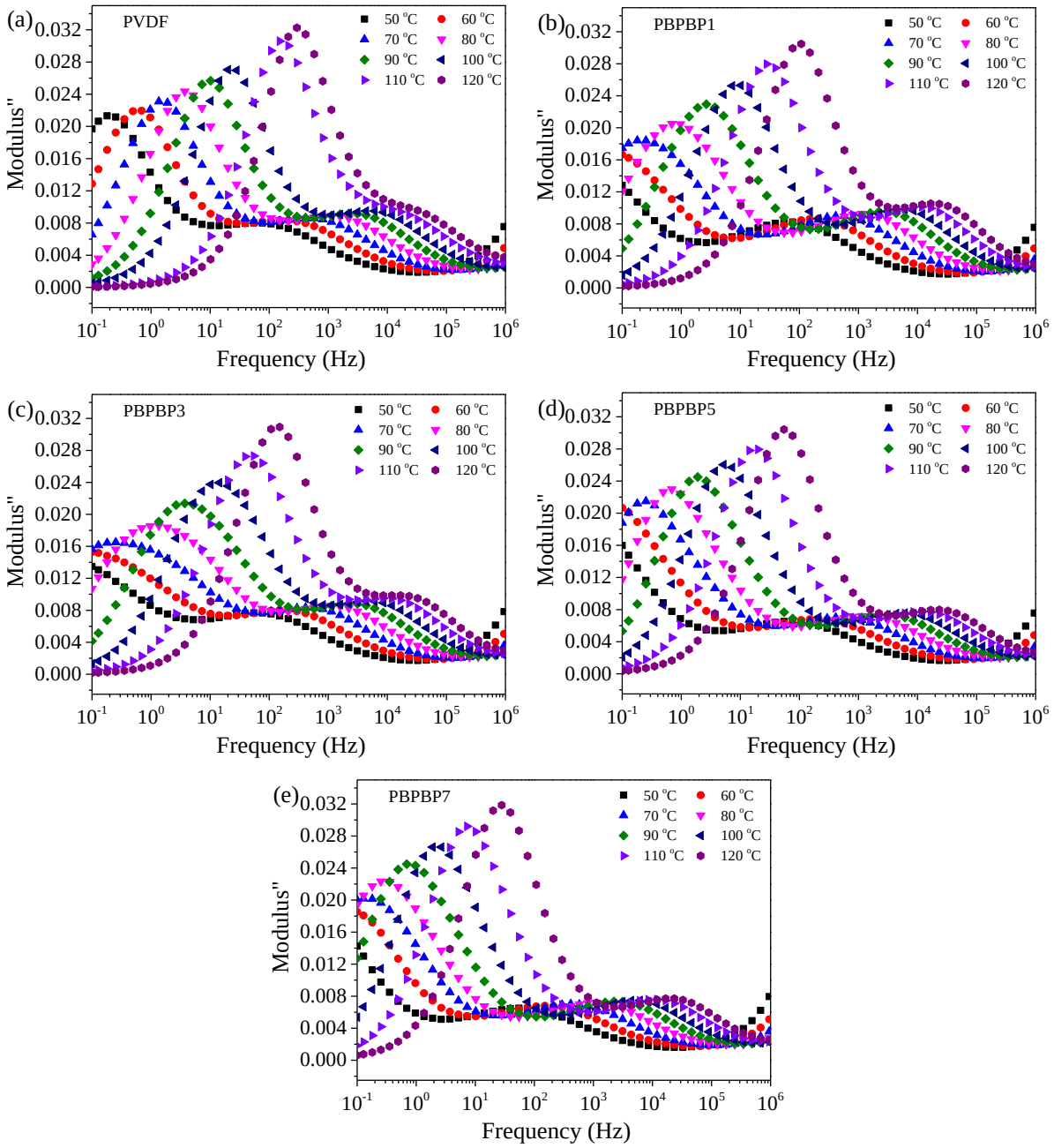

Fig. S7 The imaginary part of electric modulus (M") as a function of frequency under various temperature of **a** PVDF, **b** PBPBP1, **c** PBPBP3, **d** PBPBP5, and **e** PBPBP7, respectively

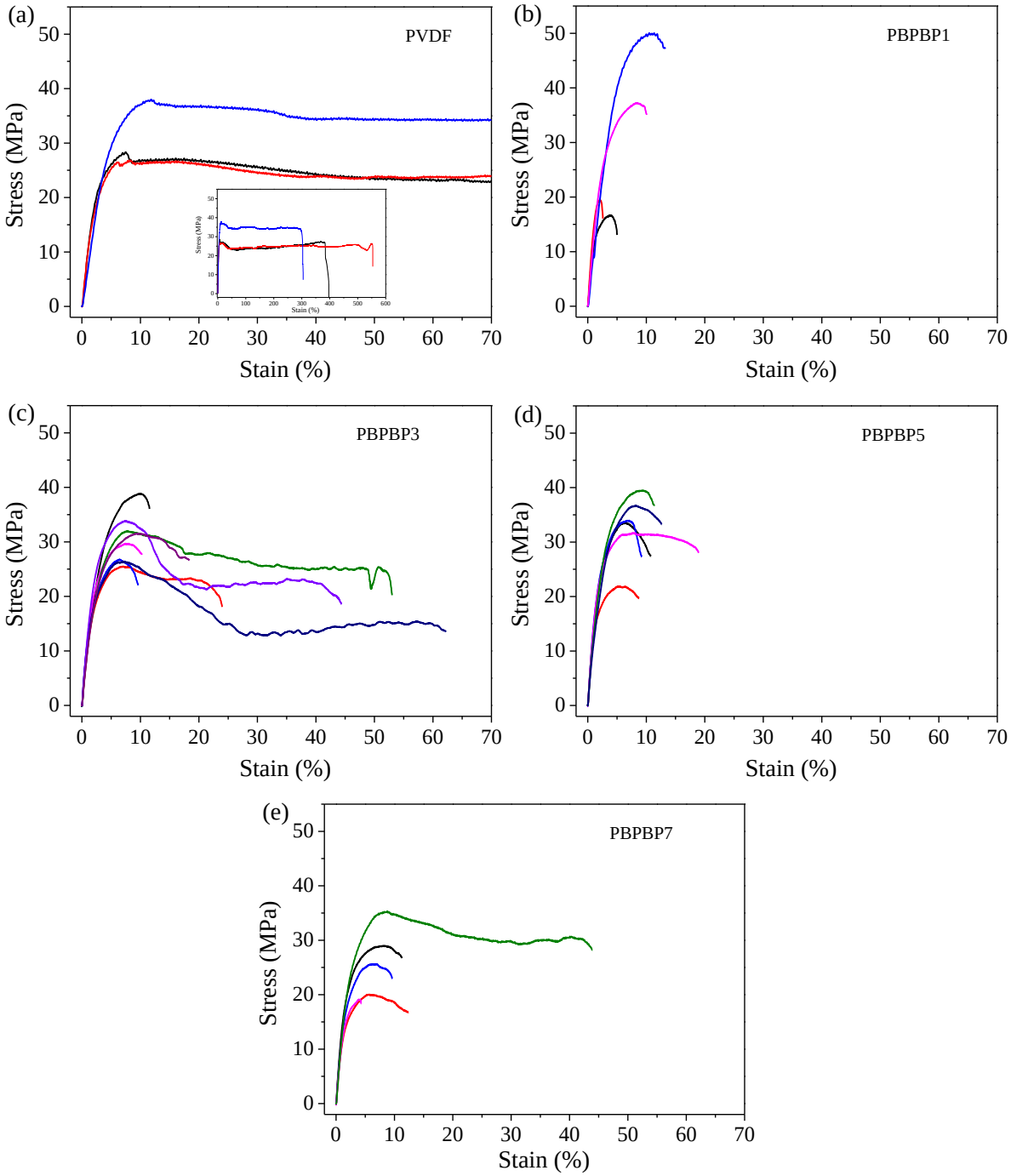

Fig. S8 The stress-strain curves of PVDF and PBPBP films

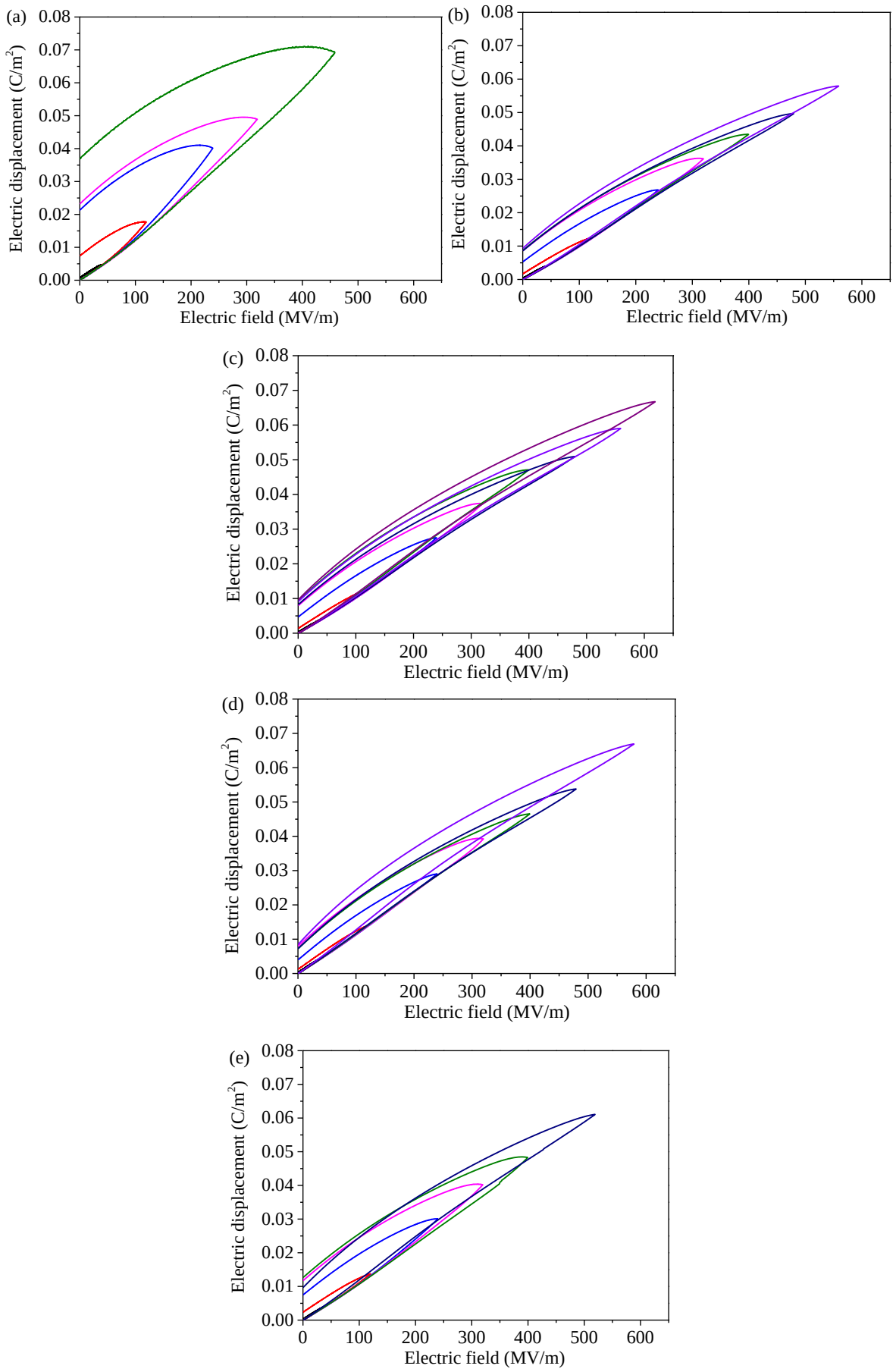

Fig. S9 D-E loops of **a** PVDF, **b** PBPBP1, **c** PBPBP3, **d** PBPBP5, and **e** PBPBP7, respectively

Table S2 Electronic property parameters of BNNS and PVDF calculated by the first-principles calculations

Materials	Electronic property parameters		
BNNS	Vacuum level	E_{vac}	5.961
	Conduction band	E_{CB}	7.141
	Valence band	E_{VB}	2.825
	Work function	φ	5.540
	Fermi level	E_F	3.040
PVDF	Vacuum level	E_{vac}	5.200
	LUMO level	LUMO	-0.224
	HOMO level	HOMO	-6.852
	Work function	φ	7.861
	Fermi level	E_F	-6.602

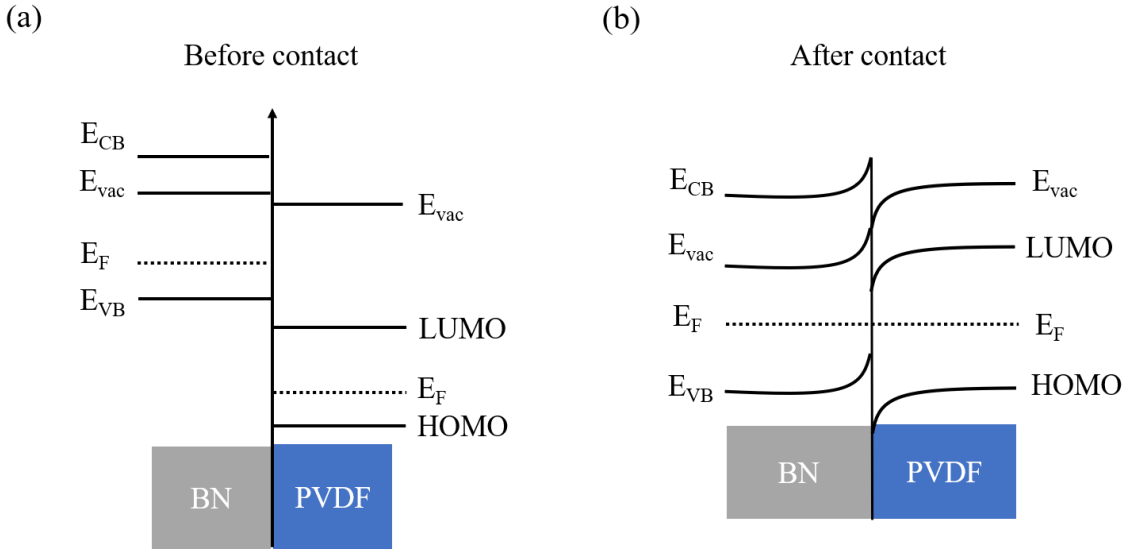

Fig. S10 Energy band strcuture of BN and PVDF, (**a**) before contact and (**b**) after contact

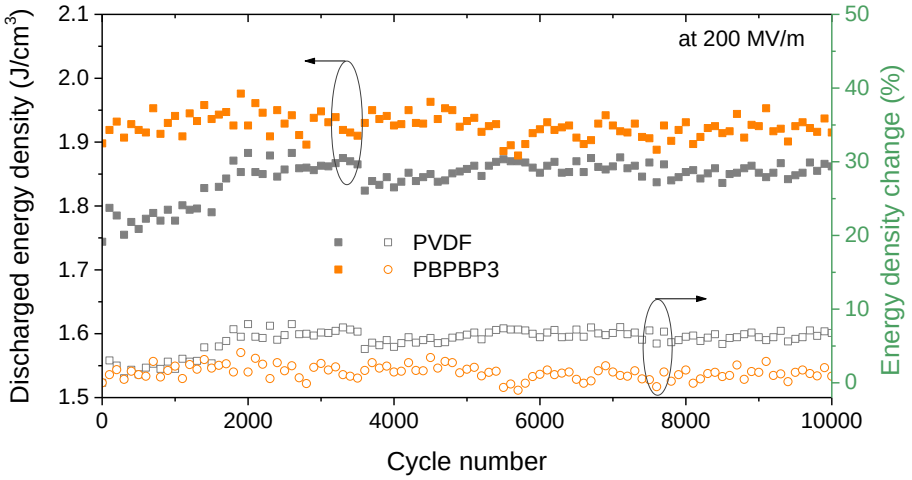

Fig. S11 Cyclic charge-discharge stabilities of PVDF and PBPBP3 under 200 MV m^{-1}